HYBRID NANOCOMPOSITES OF METHYLCELLULOSE: PHYSICO-CHEMICAL AND ANTIMICROBIAL PROPERTIES

MURODKHON RASHIDKHONOVICH KODIRKHONOV,[*]
NOIRA RAKHIMOVNA VOKHIDOVA,[**] SAYYORA SHARAFOVNA RASHIDOVA,[**]
XUAN NIE[***] and JAMSHIDKHON KADIRKHANOV[***]

[*]*Namangan State University, 316, Uychi Str., Namangan 160136, Uzbekistan*
[**]*Institute of Chemistry and Physics of Polymers of Academy of Sciences of the Republic of Uzbekistan, 7b, A. Kadiry Str., Tashkent 100128, Uzbekistan*
[***]*Department of Polymer Science and Engineering University of Science and Technology of China, Hefei, Anhui 230026, China*
✉*Corresponding author: M. R. Kodirkhonov, kodirkhonov@mail.ru*

Received October 1, 2022

Stabilized silver nanoparticles were obtained in the presence of a reducing agent – $NaBH_4$ and a stabilizer – methylcellulose, at 40 °C and pH = 5.35-11. The stabilizing role of the polymer is shown, as it prevents the oxidation and agglomeration of nanoparticles. It was found that the synthesis pH is an important factor in the formation of stable nanoparticles, which contributes to the regulation of their hydrodynamic radius. The results of UV spectroscopy established that the synthesized samples of silver nanoparticles achieve aggregative stability within 96 hours. Solutions and films of hybrid nanocomposites were comprehensively investigated by spectral, XRD and thermal studies. The diffractogram of silver NPs, corresponding to JCPDS No. 04-0783, was confirmed by the XRD method. In the studied pH range, the hydrodynamic radius and distribution of Ag NPs in methylcellulose solutions had a polymodal character, and an increase in pH to 9–11 led to an increase in particle aggregation. It was found that stabilized silver nanoparticles showed antimicrobial activity against microorganisms – *Streptococcus salivarius*, *Staphylococcus saprophyticus*, *Streptococcus mitis* and *Proteus vulgaris*, with the formation of an inhibitory zone in the range of 15.0±0.2÷20.0±0.4 mm. The synthesized samples are of applied interest in the development of antibacterial drug systems.

Keywords: methylcellulose, silver nanoparticles, hybrid nanocomposite, hydrodynamic radius, aggregative stability, antimicrobial activity

INTRODUCTION

Currently, many methods are used for the synthesis of Ag NPs, such as chemical, physical, photochemical, and biological, each with its merits and demerits. Currently, research is underway on synthetic approaches to obtaining stabilized metal nanoparticles (NPs), which are aimed at solving problems associated with cost, stability, scalability, particle size, and distribution.[1-5]

The synthesis of stabilized metal NPs is a multifactorial process, in which each factor, such as the concentration and ratio of the precursor, the chemical nature of the reducing agent and stabilizer, temperature, pH, and others, has a role to play in controlling the morphology, size, shape, distribution and performance properties of NPs; the mechanism of interaction of NPs is substantiated with biological systems.[6-11]

Silver nanoparticles were synthesized using *Capparis moonie* fruit extract. Particle size varied depending on the pH and concentration of silver nitrate. Silver NPs were tested for antibacterial and antifungal activity. All samples showed both antifungal and antibacterial activities. It was found that the activity increases with a decrease in the size of nanoparticles.[12]

Other authors obtained spherical chitosan-silver nanoparticles, with an average particle size of 13.31±0.07 nm, by reducing silver ions with *Carica* papaya extract, which had strong antibacterial properties. According to the experiments, it was found that the mechanism of the biological activity of NPs depends on the

strong interaction of Ag–CS (chitosan) with bacterial cells, the NPS being responsible for the death of bacterial cells.[13]

Hemo- and cytocompatible composite films of chitosan/cellulose sodium sulfate (CS/NaCellS) were incorporated into silver nanoparticles (AgNP) for wound treatment. It was shown that the composite film with a mass ratio of CS/NaCellS = 2:1 had a porous structure, with a porosity of 82.40±1.05%. The CS/NaCellS/AgNPs composite film showed excellent antibacterial properties against *E. coli* and *S. aureus*. The hemolysis rate of the CS/NaCellS/AgNPs composite film is less than 5%, which can be considered as meeting the requirements for biomedical materials.[14]

In recent years, green synthesis of nanoparticles using plant extracts has been used and has been successfully applied in various fields. Green synthesis of biogenic AgNPs by reduction with *Ficus religiosa* bark extract was carried out and used as an effective sorbent for the purification of chromium in wastewater, with an efficiency of more than 75%. It was found that, under the selected synthesis conditions, face-centered cubic NPs were formed, with a UV-vis absorption band at 448 nm.[15]

Silver nanoparticles coated with chitosan (CS-Ag) were obtained using $AgNO_3$ and sodium borohydride. CS-Ag has been used to sorb cadmium (Cd^{2+}) at 22 °C. Considering isothermal adsorption according to the Langmuir and Freundlich models, the maximum monolayer adsorption capacity and sorption intensity were established, and found to be equal to 119.04 mg/g and 1.6, respectively. It has been shown that NPs were stabilized due to the chemisorption of Ag on the surface of chitosan.[16]

The development of new technologically optimal *in situ* synthesis methods for obtaining hybrid nanocomposites has an advantage over *ex situ* top-down mixing methods in that it provides control of particle parameters and properties of nanomaterials. The interaction between polymer chains and inorganic nanoparticles leads to the appearance of extremely effective properties due to the synergistic effect.[17]

Despite the variety of synthesis methods, Ag NPs exhibit special physical, chemical, and mechanical properties, compared to their macroscale counterparts. This is primarily due to their small size and hence, the exceptionally effective surface area of these materials. At present, achievements in the field of synthesis, stabilization, and production of Ag NPs have contributed to the emergence of a new generation of commercial products and an increase in the number of fundamental researches in the field of nanotechnologies.[18] The physical and chemical properties mentioned above make AgNPs suitable for a variety of new commercial and technological applications, including antiseptics in medicine, cosmetics, food packaging, bioengineering, electrochemistry, and catalysis. The fact that the importance of metal nanoparticles is increasing in various fields, such as nano-catalysis, materials with improved electronic, magnetic, mechanical, and optoelectronic properties, as well as medical, cosmetic, and agricultural preparations, the use of various nano-compounds for the environment, the textile industry, *etc*. shows the value and importance of the synthesis of metal nanoparticles, among which the development of methods for obtaining silver particles will play a dominant role. The stabilization of Ag NPs by polymers with their bioactive properties has great prospects in the scientific and applied aspect due to the manifestation of synergistic effects.[18-20]

The development of new nano-preparations based on non-toxic, biocompatible, and biodegradable polysaccharides remains an urgent scientific problem. The inclusion of silver nanoparticles into a polymer matrix yields a material with antimicrobial activity, while choosing a cellulose derivative as polymer matrix brings additional advantages, such as renewability of the raw material, water solubility and low cost, yielding materials with increased environmental and economic value. The present work aims to obtain stabilized silver nanoparticles and use them in the development of a hybrid methylcellulose-based nanocomposite material, with bactericidal properties. The effect of pH on the hydrodynamic parameters and physical-chemical properties of Ag NPs was studied. The prepared materials were investigated by spectral, XRD and thermal analyses.

EXPERIMENTAL

Materials

Silver nitrate ($AgNO_3$, 99.8%), sodium borohydride ($NaBH_4$, 98%), and methylcellulose (MC, molecular mass 102×10^3 and degree of substitution 584) were purchased from Sigma-Aldrich, BR.

Methods

DLS was used to measure the particle size of composites. The range of measured dimensions is in

the range from fractions of nm to 5-10 microns. The power of the analyzer's laser is in the range of 2 mW-35 mW. Photocor analyzers have a mode of automatic measurements, processing, and presentation of analysis results.

UV-spectroscopic studies were carried out with a Specord 210 spectrophotometer in the range of 190-1000 nm. The accuracy of UV photometry with potassium dichromate was ±0.01, complying with Ph. Eur.

Thermal analysis was performed on an STA PT1600 Synchronous Thermal Analyzer from LINSEIS (Germany), using thermogravimetry (TG) and DTG methods. The measurements were carried out in air atmosphere in dynamic mode, with a heating rate of 10 °C/min, in the temperature range of 0–800 °C. The sample weight was 14.4 mg.

X-ray studies were carried out based on diffraction patterns, which were taken on a computer-controlled Mini Flex 600 (Rigaku, Japan). We used CuKα radiation (β-filter, Ni, 1.54178 current modes and tube voltage 15 mA, 40 kV) and a constant detector rotation speed of 10 °C/min, with a step of 0.02 °C, and a scanning angle from 3 to 90°. The average crystallite size was calculated using the Debye-Scherrer formula.

IR Fourier spectroscopic studies of the obtained samples were carried out on an IRTracer-100 spectrometer from Bruker (Germany). The IRTracer-100 is characterized by a high signal-to-noise ratio of 60,000:1, a resolution of 0.25 cm^{-1}, and the ability to work in fast scanning mode with the registration of up to 20 spectra per second.

The biologically active properties of nanoparticle solutions concerning gram-positive and gram-negative microorganisms were studied by the disk-diffusion method in an agar-agar nutrient medium, using paper disks impregnated with solutions.[21]

RESULTS AND DISCUSSION

Synthesis of silver nanoparticles and their identification

The synthesis of stabilized Ag NPs was carried out by the method of chemical reduction at t = 40 °C, at a molar salt concentration $[Ag^+] = 1.05\times10^{-3}$ mol/L and reducing agents $[NaBH_4] = 5.25\times10^{-4}$ mol/L. The formation of Ag NPs occurs both in the presence and in the absence of a stabilizer – methylcellulose macromolecules. A scheme of the formation and stabilization of silver nanoparticles surrounded by a polymer shell is shown in Figure 1.

Silver NPs were formed in aqueous solutions of silver nitrate by reacting silver ions with sodium borohydride at 40 °C, the molar ratio $[Ag^+/NaBH_4] = 2$, and stirring the $NaBH_4$ solution at a rate of 5 µL/min. Stabilization occurs by the chemisorption of silver nanoparticles on the surface of methylcellulose, which prevents their agglomeration and oxidation.

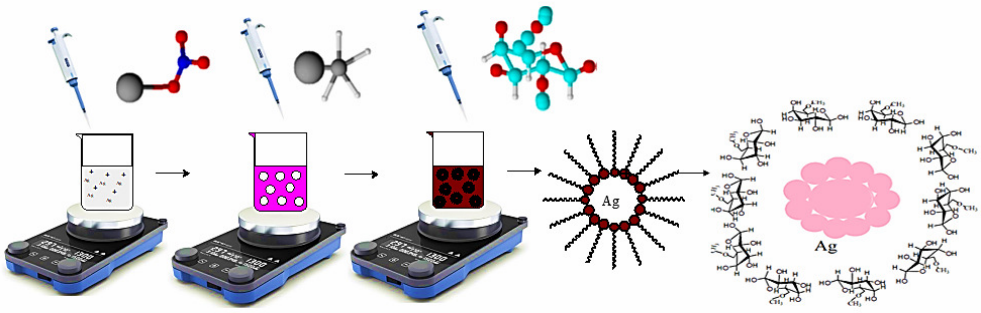

$AgNO_3+NaBH_4+H_2O = NaNO_3+B(OH)_3+H_2+Ag$

Figure 1: Schematic representation of the synthesis and stabilization of AgNPs obtained using the method of chemical reduction in the presence of methylcellulose

Synthesis of Ag nanoparticles under *ex situ* conditions

Silver NPs were obtained in the absence of a stabilizer under "*ex situ*" conditions, and solutions were studied by the UV spectroscopic method. It can be seen from the spectrum that the interaction of silver ions with sodium borohydride results in the formation of a light pink colloidal solution (Fig. 2).

The presence of a characteristic absorption band at λ_{max} = 275 nm indicates that Ag_n clusters are formed as a result of the redox reaction. However, the absence of a stabilizing agent in the system leads to rapid oxidation and agglomeration of NPs, as a result of which the color of the

solution changes from pink to dark brown, and the bulk metal precipitates. The hydrodynamic parameters of AgNPs were measured on a DLS instrument (Fig. 3). It was shown that 92.4% of the nanoparticles had a radius of 76.2 nm, and the proportion of aggregated particles with a radius of 2.8×10^5 was 7.6%. It should be noted that the low value of $\chi = 3.2\times10^{-4}$ also shows the reliability of the obtained data.

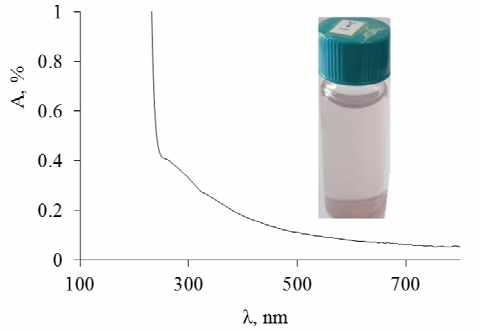

Figure 2: UV spectrum and photograph of a solution containing AgNPs obtained in the absence of a stabilizer; $[Ag^+] = 1.05\times10^{-3}$ mol/L, $[NaBH_4] = 5.25\times10^{-4}$ mol/L

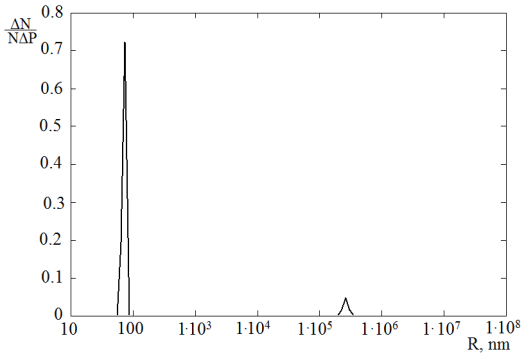

Figure 3: Hydrodynamic radius of silver nanoparticles obtained at t = 40 °C and $[Ag^+] = 1.05\times10^{-3}$ mol/L, $[NaBH_4] = 5.25\times10^{-4}$ mol/L

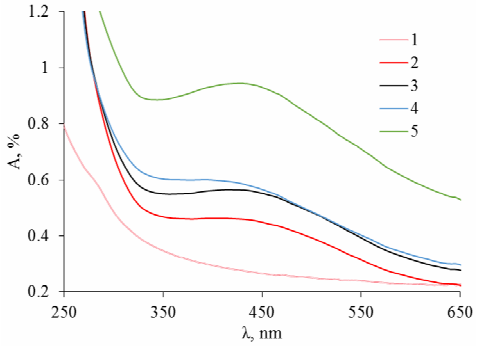

Figure 4: UV spectra of stabilized MC-Ag NPs obtained at different pH values: 1) MC, 2) pH 5.32; 3) pH 6.5; 4) pH 9.0; 5) pH 11

Ag NPs obtained *in situ*. Characterization of hybrid MC-Ag nanocomposites

UV spectroscopy

To obtain stabilized Ag NPs, the synthesis was carried out *in situ*, in the presence of methylcellulose, with varying pH of the medium (Fig. 4).

It can be seen that, in contrast to the spectra of MC-Ag, the UV spectrum of MC lacks an absorption band at 350–650 nm (Fig. 4, line 1). As the results show, the rest of the studied samples (Fig. 4, lines 2-5) show clearly defined plasmonic absorption bands at λ_{max} = 425-435 nm, which characterize Ag NPs up to 100 nm in size. It was found that, with an increase in the pH of the medium from 5.32 to 11, a shift of the absorption bands by approximately 10 nm is observed, and, accordingly, their intensity increases, as well as the color saturation of the MC-Ag solutions. These absorption maxima tend to shift to longer wavelengths and become broader, indicating aggregation and formation of larger radius silver particles. The formation of a colloidal solution of dark orange color indicates the aggregation of NPs to a large extent. The stability of suspended nanoparticles is related to the presence of a polymer in the system.

XRD analysis

Figure 5 shows X-ray diffraction patterns of MC and MC-Ag films obtained by the reduction

of silver ions with sodium borohydride at pH 6.5. To reveal the formation of Ag NPs and the optimal composition of the reaction products of silver nitrate with $NaBH_4$ in the presence of methylcellulose, an X-ray phase analysis was carried out (Fig. 5). The X-ray diffraction pattern of the MC powder shows broad diffraction peaks at 2θ = 9° and 19.86°, which can be attributed to the (110) and (020) crystal lattices, respectively.

As has been previously established,[22-24] a characteristic reflex associated with methoxy-substituted cellulose units is observed at an angle of 2θ = 9°, while a reflex at 2θ=19° appears due to chains of unsubstituted cellulose. The increased intensity indicates high crystallinity of the polymer matrix.[25,26] A slight shift of the characteristic reflection of MC to 2θ = 19.86° indicates the presence of H-H bonds and electrostatic molecular interactions between the electron donor groups of MC. As can be seen from Figure 5, the characteristic reflections of the hybrid nanocomposite MC-Ag are observed at angles 2θ = 36°, 44°, 64.5°, 78°, and 82°, and can be assigned to Ag (111), Ag (200), Ag (220), Ag (311) and Ag (222), respectively. The intensity of the reflections of each phase depends on the amount in the mixture under study. The characteristic peaks of Ag NPs are in good agreement with JCPDS #04-0783.[27] The X-ray diffraction pattern of MC-Ag has a weak but broad peak characterizing the cellulose units of MC at an angle of 2θ = 19.86°. During the stabilization of silver NPs, the ordered structure of the macromolecule is disturbed, which leads to the disappearance of the reflection at the angle of 2θ = 9°. The proposed mechanism for the reduction of silver ions with sodium borohydride in the presence of a polymer is presented in Figure 1, discussed above.

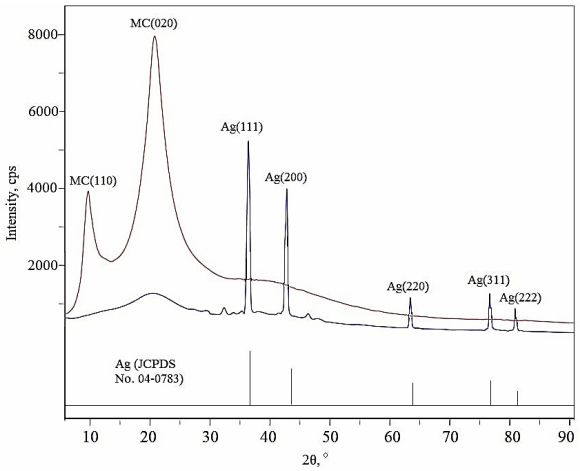

Figure 5: X-ray pattern of MC films and hybrid MC-Ag nanocomposite obtained at pH 6.5

Table 1
Some parameters of methylcellulose crystallites and MC-Ag hybrid nanocomposite obtained at pH 6.5

			MC		
#	2θ	d, Å	β, °	D, nm	D average, nm
1	8.99	10.06	1.58	5.28	4
2	19.86	4.47	2.93	2.87	
			MC-Ag		
1	27.06	3.292	0.560	15.3	21
2	28.60	3.119	0.360	23.5	
3	35.81	2.506	0.260	33.5	
4	43.98	2.150	0.300	29.6	
5	45.70	1.984	0.540	16.6	
6	64.51	1.482	0.255	38.1	
7	77.84	1.253	0.216	48.6	
8	82.09	1.197	0.207	52.4	

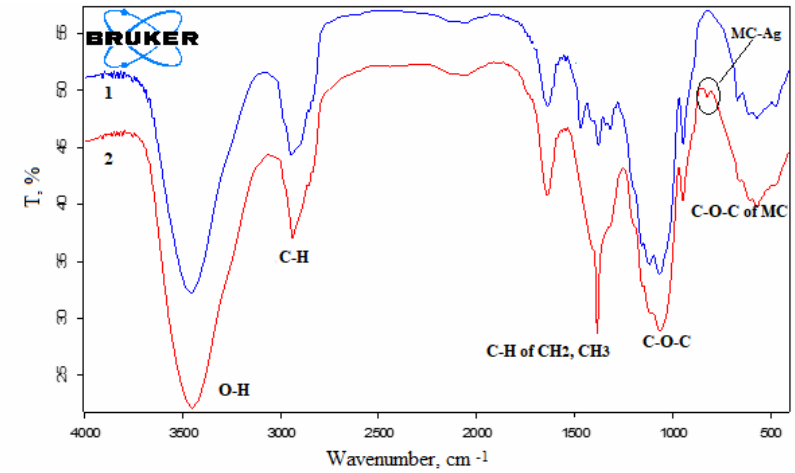

Figure 6: FTIR spectra of samples of methylcellulose (1) and hybrid nanocomposite MC-Ag (2)

According to the Debye-Scherrer formula D = 0.89λ/(β1/2cosθ), the interplanar distances of crystals and the average size of MC and MC-Ag crystallites were calculated (Table 1).[28]

It was found that the size of MC crystallites is from 2.9 to 5.3 nm (D average = 4 nm), while for the MC-Ag nanocomposite, the crystallite diameter varies from 15.3 to 52.4 nm (D average = 21 nm). The results indicate that agglomeration of methylcellulose crystallites takes place in polymer solutions.

FT-IR spectroscopy

Figure 6 demonstrates the IR spectra of methylcellulose samples (1) and MC-Ag NPs (2) obtained at pH 6.5.

It is known that the infrared spectra of cellulose and methylcellulose have significant differences in the regions from 3600 to 2700 cm-1 and from 1500 to 800 cm-1. The ratio between the absorption intensity of the OH (~3400 cm-1) and CH (~2900 cm-1) bands in the spectra of methylated samples is lower than in the spectrum of cellulose, which indicates methylation of some units.26,29

A broad absorption band with a minimum at 3450 cm-1 corresponds to hydroxyl groups and H–H bonds between the electron donor groups of MC (Fig. 6). The presence of absorption bands at 2946-2853 cm–1 is due to stretching vibrations of the C–H groups of glycosidic cycles; the absorption band observed at about 944 cm^{-1} corresponds to the –C–H bending vibrations of MC groups. The absorption band at 1066 cm^{-1} characterizes the presence of deformation vibrations of the –C–O–C– ester groups of the polymer. When comparing the spectrum of methylcellulose with the spectrum of MC-Ag, the main observed changes consisted in a decrease in the intensity of the bands corresponding to -OH groups at 2933 cm^{-1}, a combination and the formation of intense peaks in the regions 1408-1383 cm^{-1} of the stretching vibrations of the C–H groups and bending vibrations of the ester groups C–O–C at 669 cm^{-1} by 14 cm^{-1}. It should be noted that the absorption band of C-H groups in MC at 1317 cm^{-1} in the spectrum of MC-Ag is shifted by 66 cm^{-1}. A weak shoulder at 823 cm^{-1} is also observed, which is associated with the introduction of silver NPs into the polymer matrix. Such changes indicate the participation of methylcellulose macromolecules in the stabilization of AgNPs.

TG and DTG studies

The stability of the hybrid MC-Ag nanocomposite was studied by thermogravimetry and DTG analysis in the temperature range of 0–800 °C in the air (Fig. 7).

As can be seen in Figure 7 (a), the beginning of the thermal decomposition of the studied samples of MC and MC-Ag occurs up to 100 °C caused by the desorption of adsorbed moisture and solvent traces. For the initial methylcellulose, the weight loss is of 3 wt% at 76.1 °C, and for the hybrid nanocomposite obtained on its basis, an increase in the weight of the sample by 19, 16, and 13 wt% is observed at 63.8, 192.4, and 233.6 °C, respectively. The increase in the mass of the sample is possibly associated with the partial

formation of metal oxide in the atmosphere of atmospheric oxygen. At 250.8 °C, the entire MC film decreases by 6 wt% of the total sample weight, and at 289.5 °C, the nanocomposite underwent a weight loss of 13 wt%, which indicates the onset of thermal degradation of the polymer matrix. A significant decrease in the weight of the MC sample by 79% at 344.9 °C is associated with the decomposition of the polymer, whereas for the MC-Ag nanocomposite, such a change occurs at 429.8 °C, with a decrease in weight by 71 wt%. It can be seen that the introduction of Ag NPs into the polymer matrix increases the degradation temperature of MC by 85 °C. This indicates the higher thermal stability of the new methylcellulose nanocomposite developed by inclusion of silver nanoparticles into the polymer matrix.

The intense DTG curves of the MC sample at 85.3 °C and 309.2 °C indicate that moisture evaporation and polymer degradation proceed at a rate of 0.6 %/min and 15 %/min, respectively. It should be noted that the desorption rate proceeds at a significantly low rate (0.6 %/min). When heated above 358.8 °C, no weight loss of the MC sample occurs. At the same time, the total weight loss was about 88%, which indicates the presence of moisture in the MC. According to the results obtained, for the MC-Ag films obtained in this work, there are 3 stages with maxima at 215.1 °C, 289 °C, and 399 °C, which proceed at rates of 0.6, 9.18, and 3.9 %/min. These changes are associated with the presence of methylcellulose in the composite. The total weight loss is equal to 84 wt%. Thus, it was found that the obtained hybrid MC-Ag nanocomposites exhibit increased thermal stability compared to the initial polymer matrix, MC.[30]

DLS measurements

To study the effect of methylcellulose macromolecules on the stabilization of silver nanoparticles, the hydrodynamic radius of polymer particles was measured (Fig. 8).

From the results of DLS measurements, it was revealed that the hydrodynamic radius of 96% of the particles of MC macromolecules is 100 μm, and the radius of 4% of the particles is 0.1–8.7 nm. The large particle radius is associated with the formation of intra- and intermolecular H-H bonds, which contribute to the aggregation of polymer chains.

The effect of MC on the size and distribution of polymer-stabilized silver nanoparticles was studied (Fig. 8 a and b). NPs were synthesized in the pH range from 5.32 to 11, *i.e.*, from weakly acidic to strongly alkaline media. It was found that the formation of NPs in all samples has a polymodal character; nanoparticles with a large spread of particles are formed. At $[Ag^+]/[MC]$ = 11, the particle size of MC decreases >50 times more than the hydrodynamic radius of the original polymer.

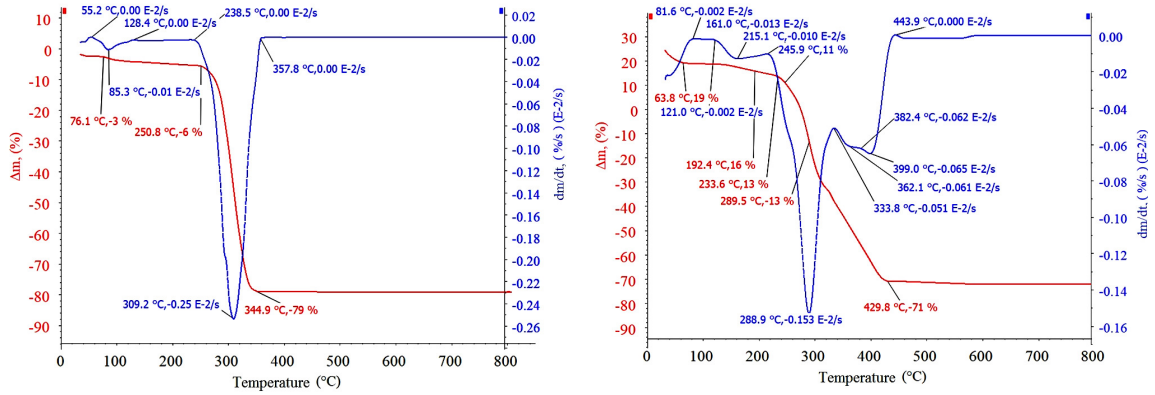

(a) (b)

Figure 7: Thermal gravimetric and differential thermogravimetric analyses of MC samples (a) and MC-Ag hybrid nanocomposite (b)

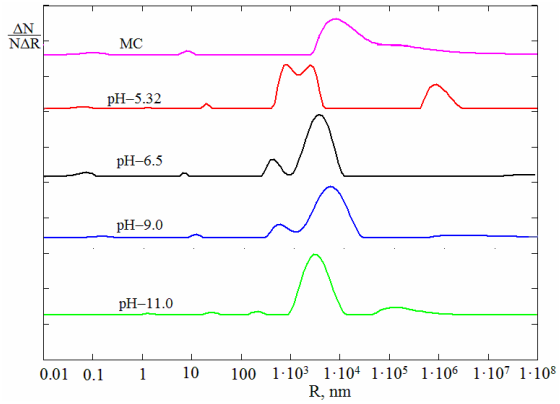

Figure 8: Hydrodynamic radius and distribution of NPs in solutions of methylcellulose and MC-Ag obtained at t = 40 °C; $[Ag^+/MC]$ = 11 wt. cor.; $[Ag^+]/[NaBH_4]$ = 2; $[Ag^+]$ = 1.05×10^{-3} mol/L and various pH values

It should be noted that in the process of stabilization at all pH values of the synthesis, the distribution of particles over the polymer matrix has a polymodal character. For example, at pH = 5.32, the hydrodynamic particle size was 21 nm (2%); 890 nm (32%); 2.5 µm (40%), 100 µm (25%); when at pH = 6.50, there is a large spread of particles – 12 nm (2.3%), 542 nm (11%), 5.5 µm (79.4%), macroparticles – 7.3%. With an increase in pH from 9 to 11, an increase in the proportion of macroparticles is observed: 8 nm (4.6%), 517 nm (11.4%), 4.5 µm (80%), macroparticles – 4.6%; and 25 nm (2.2%), 200 nm (2%), 3.3 µm (82%), macroparticles – 14%, respectively. For all measurements, the value χ^2 was equal to 3×10^{-3} ±2.002.

Study of the aggregative stability of MC-Ag NPs

Ag NPs, which are stable over time, are of fundamental and applied interest in the creation of antibacterial drugs based on them. The choice of methylcellulose as a stabilizer is due to its water solubility, non-toxicity ($LD_{50}\geq10.000$ mg/kg), biocompatibility, and biodegradability, which provides the creation of a potential antimicrobial drug. In this regard, the aggregative stability of solutions of MC-Ag NPs for 0-96 hours was studied (Fig. 9).

Ag solutions in a certain time interval show that under the chosen synthesis conditions, the reduction of silver ions continues and the saturation of the solution color increases from light beige to dark brown.

As the results show (Fig. 10), the intensity of the absorption bands at λ_{max} = 275 nm and λ_{max} = 475 nm decreases proportionally with time, which may be associated with the formation of agglomerates up to macroparticles. It should be noted that after the 4th day, the solution was stable, and no precipitation was observed. The size and distribution of NPs were studied by the DLS method (Fig. 11).

The results indicate that the formation of polymer-stabilized Ag NPs continues for several days, after which the particle size and color of the solutions remain stable. It has been established that the hydrodynamic radius of 96% of the particles of the sample obtained at pH = 5.32 is 5.8 µm, and that of 4.1% is 205 nm, while for the MC-Ag sample with pH = 6.5 the radius of 70% of the particles is 4.25 µm, that of 25.4% is 120 µm and that of 4.6% NPs had a 268 nm radius.

It was found that the distribution of MC-Ag particles synthesized at pH = 9 had a polymodal character, since particles with a hydrodynamic radius from 2 nm to 1 mm were formed in the solution. In particular, 13% of the particles had a radius of 1 mm, 71% of the particles had a radius of 2.7 µm, and 8.8% of the particles had a radius from 2 to 232 nm.

At pH 11, with increasing time to 96 h, the radius of 78.5% of the particles was 4.8 µm, that of 17.1% – 3.5 mm, and of 4.5% – 5-70 nm. The results indicate that in all the studied solutions, within 0-96 hours, agglomeration of particles certainly occurs, despite this, the solutions of MC-Ag remain aggregately stable.

Antimicrobial properties of MC-Ag NPs

The antimicrobial activity of the synthesized sample of the hybrid nanocomposite MC-Ag was studied concerning several gram-positive and gram-negative pathogenic microorganisms that cause various diseases in living organisms (Table

2). Results show that both acetic acid and 0.5% solutions of hybrid nanocomposites MC-Ag effectively prevent the growth and development of spherical and rod-shaped pathogens with the formation of an inhibition zone in the range of 8.0±0.1÷13.0±0.2 mm and 15.0±0.2 ÷ 20.0±0.4 mm, respectively.

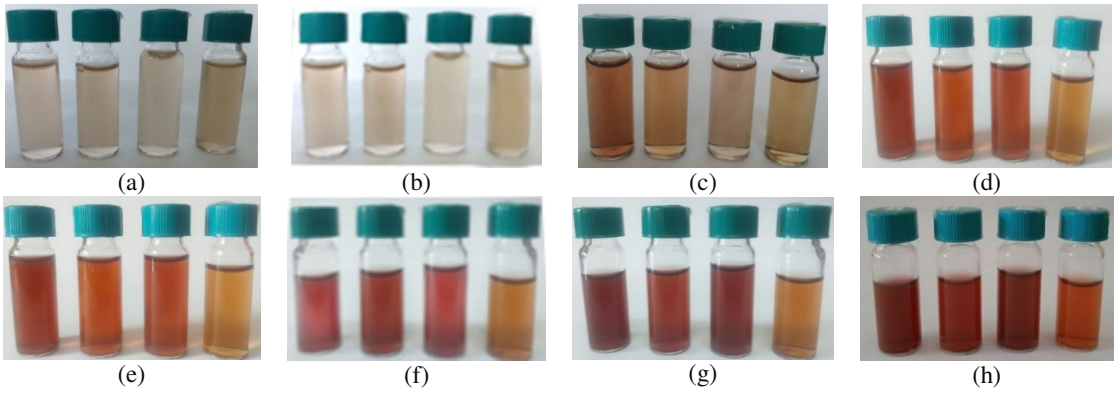

Figure 9: Effect of time on the aggregative stability of solutions of Ag NPs stabilized by MC macromolecules, pH 6.5; (a) 0 h; (b) 5 h; (c) 19 h; (d) 27 h; (e) 45 h; (f) 55 h; (g) 75 h; (h) 96 h

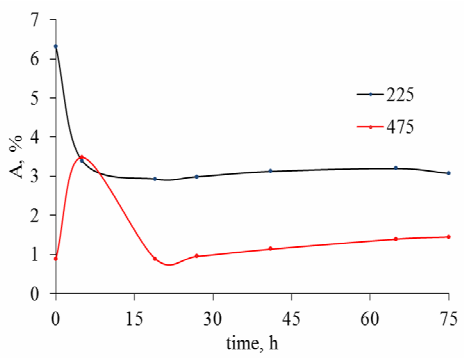

Figure 10: Effect of time on optical density ($D_{225\ nm}$ and $D_{475\ nm}$) of MC-Ag NPs solutions obtained at pH = 6.5

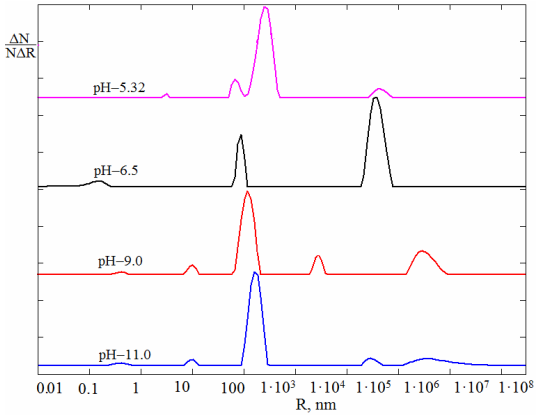

Figure 11: Hydrodynamic radius and distribution of MC-Ag NPs obtained at t = 40 °C; [Ag^+/MC] = 11 wt cor.; [Ag^+]/[$NaBH_4$] = 2; [Ag^+] = 1.05×10^{-3} mol/L and various pH values after 96 hours

Table 2
Sensitivity of microbes to synthesized methylcellulose-silver composites under *in vitro* conditions (M±m) mm

#	Pathogenic microbes	Sterile zone, mm	
		CH_3COOH	NPs MC-Ag
1	*Streptococcus salivarius*	10.0 ±0.1	15.0±0.2
2	*Staphylococcus saprophyticus*	8.0 ± 0.1	15.0±0.2
3	*Streptococcus mitis*	13.0 ± 0.2	15.0 ±0.2
4	*Proteus vulgaris*	10.0 ± 0.1	20.0±0.4

It was found that when exposed to bacterial strains *Streptococcus salivarius*, *Staphylococcus saprophyticus* and *Streptococcus mitis*, the solutions of MC-Ag NPs contributed to the formation of a sterile zone of 15.0±0.2 mm, with the highest activity against rod-shaped microorganisms – *Proteus vulgaris*, which cause wound infections in the intestines of humans and animals. It has been established that acetic acid

has weak, while MC-Ag hybrid nanocomposites exhibit moderate antimicrobial properties.

To conclude, the results of the study indicate that the obtained hybrid nanocomposites are of interest in the development of biological products with increased antibacterial activity. Our research in this direction is currently ongoing.

CONCLUSION

Thus, we have synthesized polymer-stabilized silver NPs by adjusting the pH of the medium from 5.3 to 11 under *in situ* conditions. The hydrodynamic parameters of MC macromolecules and MC-Ag hybrid nanocomposites were determined. It was found that the polymer methylcellulose effectively stabilizes NPs from oxidation and agglomeration. It was found that the pH of the synthesis contributes to the production of NPs with controlled size and distribution over the polymer matrix. It was found that the obtained NPs at t = 40 °C; $[Ag^+/MC]$ = 11 wt. cor.; $[Ag^+]/[NaBH_4]$ = 2; $[Ag^+] = 1.05\times10^{-3}$ mol/L and various pH values are aggregately stable for 96 hours. The obtained hybrid composites were identified by UV and IR spectroscopy, XRD, DLS, TG and DTG analyses. The presence of silver NPs corresponding to JCPDS #04-0783 was confirmed by XRD analysis. In the pH range of 5.35–11, the hydrodynamic radius and distribution of Ag NPs in the methylcellulose solutions had a polymodal character, and an increase in pH to 9–11 led to an increase in particle aggregation. Thermal analysis showed that the introduction of silver nanoparticles into the MC macromolecule contributes to an increase in their thermal stability. Solutions of polymer-stabilized nanoparticles effectively suppressed the growth and development of gram-positive and gram-negative pathogens – *Streptococcus salivarius*, *Staphylococcus saprophyticus*, *Streptococcus mitis* and *Proteus vulgaris*, forming an inhibition zone of up to 20.0 ±0.4 mm. Solutions of MC-Ag are of interest in the development of novel, non-toxic and biodegradable drug systems.

REFERENCES

[1] A. Haider and I. K. Kang, *Adv. Mater. Sci. Eng.*, **1**, 165257 (2015), http://dx.doi.org/10.1155/2015/165257

[2] X. Hu, J. He, L. Zhu, S. Machmudah, W. H. Kanda *et al.*, *Polymers*, **14**, 89 (2022), https://doi.org/10.3390/polym14010089

[3] H. Chen, T. Wang, H. Shen, W. Liu, S. Wang *et al.*, *Nano Res.*, **8**, 2871 (2015), https://doi.org/10.1007/s12274-015-0792-0

[4] Y. Zhao, Y. Cheng, L. Shang, J. Wang, Z. Xie *et al.*, *Small*, **11**, 151 (2015), https://doi.org/10.1002/smll.201401600

[5] J. H. Jung, C. H. Choi, S. Chung and Y. M. Chung, *Lab. Chip.* **9**, 2596 (2009), https://doi.org/10.1039/B901308C

[6] E. O. Nasakina, E. B. Gulyaeva and M. Yu. Queen, *Advances in Chemistry and Chemical Technology*, V. XXIV, **112**, 97 (2017), (in Russian)

[7] J. Tan, S. Shah, A. Thomas, H. D. Ou-Yang and Y. Liu, *Microfluid. Nanofluid.*, **14**, 77 (2013), https://doi.org/10.1007/s10404-012-1024-5

[8] A. Albanese, P. S. Tang and W. Chan, *Ann. Rev. Biomed. Eng.*, **14**, 1 (2012), https://doi.org/10.1146/annurev-bioeng-071811-150124

[9] M. Ningning, M. Chao, L. Chuanyan, W. Ting, T. Yongjun *et al.*, *J. Nanosci. Nanotechnol.*, **13**, 6485 (2013), https://doi.org/10.1166/jnn.2013.7525

[10] V. V. Makarov, A. J. Love, O. V. Sinitsyna, S. S Makarova, I. V. Yaminsky, *et al.*, *Acta Nat.*, **6**, 35 (2014), https://doi.org/10.32607/20758251-2014-6-1-35-44

[11] D. Vollat, F. D. Fisher and D. Holek Beilstein, *J. Nanotechnol.*, **9**, 2265 (2018), https://doi.org/10.3762/bjnano.9.211

[12] B. A. Lakkappa, S. Ch. Jasmith and M. G. Prabhuodeyara, *Org. Med. Chem. Int. J.*, **3**, 555622 (2017), https://doi.org/10.19080/OMCIJ.2017.03.555622

[13] S. Samanta, J. Banerjee, B. Das, J. Mandal, S. Chatterjee *et al.*, *Int. J. Biol. Macromol.*, **219**, 919 (2022), https://doi.org/10.1016/j.ijbiomac.2022.08.050

[14] Ch. Tang, B. Zhao, J. Zhu, X. Lu and G. Jiang, *Mater. Today Commun.*, **33**, 104192 (2022), https://doi.org/10.1016/j.mtcomm.2022.104192

[15] A. Riaz, S. Nosheen and T. A. Mughal, *Microsc. Res. Tech.*, **85**, 3618 (2022), https://doi.org/10.1002/jemt.24214

[16] Z. Khan and Sh. Ahmadal-Tabaiti, *Arab. J. Chem.*, **15**, 104154 (2022), https://doi.org/10.1016/j.arabjc.2022.104154

[17] Y. Huang, J. Li, L. Zhou, Ch. Cheng, Z. Hu *et al.*, *J. Macromol. Sci., A*, **59**, 605 (2022), https://doi.org/10.1080/10601325.2022.2101924

[18] B. Calderón-Jiménez, M. E. Johnson, A. R. Montoro Bustos, K. E. Murphy, M. R. Winchester *et al.*, *Front. Chem.*, **5**, 6 (2017), https://doi.org/10.3389/fchem.2017.00006

[19] M. Khan (Ed.), "Silver Nanoparticles – Fabrication, Characterization and Application", IntechOpen, 2018, https://doi.org/10.5772/intechopen.75611

[20] P. L. Nasatto, F. Pignon, J. L. Silveira, M. E. R. Duarte, M. D. Noseda *et al.*, *Polymers*, **7**, 777 (2017), https://doi.org/10.3390/polym7050777

[21] A. K. Ojha, S. Forster, S. Kumar, S. Vats, S. Negi *et al*., *J. Nanobiotechnol*., **11**, 42 (2013), https://doi.org/10.1186/1477-3155-11-42
[22] M. Fahad, M. A. Khan and M. Gilbert, *Gels*, **7**, 205 (2018), https://doi.org/10.3390/gels7040205
[23] A. Pinotti, M. A. Garcia, M. N. Martino and N. E. Zaritzky, *Food Hydrocoll*., **21**, 66 (2007), https://doi.org/10.1016/j.foodhyd.2006.02.001
[24] T. Kondo, A. Koschella, B. Heublein, D. Klemm and T. Heinze, *Carbohyd. Res*., **343**, 2600 (2008), https://doi.org/10.1016/j.carres.2008.06.003
[25] A. M. Bochek, N. M. Zabivalova, V. K. Lavrent'ev, M. F. Lebedeva, T. E. Sukhanova *et al*., *Russ. J. Appl. Chem*., **74**, 1358 (2001), https://doi.org/10.1023/A:1013774800778
[26] N. A. Nik Aziz, N. K. Idris and M. I. N. Isa, *Int. J. Polym. Anal. Charact*., **15**, 319 (2010), https://doi.org/10.1080/1023666X.2010.493291
[27] A. S. Lanje, S. J. Sharma and R. B. Pode, *J. Chem. Pharm. Res*., **2**, 478 (2010), https://www.jocpr.com/articles/synthesis-of-silver-nanoparticles-a-safer-alternative-to-conventional-antimicrobial-and-antibacterial-agents
[28] L. I. Mirkin, "Handbook of X-Ray Diffraction Analysis of Polycrystals", Moscow, 1961, (in Russian)
[29] G. P. Rose, V. G. Filho and R. Assunção, *Carbohyd. Polym*., **67**, 182 (2007), https://doi.org/10.1016/j.carbpol.2006.05.007
[30] B. M. Liebeck, N. Hidalgo, G. Roth, K. Popescu and A. Boker, *Polymers*, **9**, 91 (2017), https://doi.org/10.3390/polym9030091